Low-lying magnetic excitations of doubly-closed-shell nuclei and nucleon-nucleon effective interactions

V. De Donno, G. Co', and C. Maieron
Dipartimento di Fisica, Università del Salento and, INFN Sezione di Lecce, Via Arnesano, I-73100 Lecce, Italy

M. Anguiano, A. M. Lallena, and M. Moreno Torres
Departamento de Física Atómica, Molecular y Nuclear, Universidad de Granada, E-18071 Granada, Spain
(Received 16 January 2009; published 21 April 2009)

We have studied the low-lying magnetic spectra of ^{12}C, ^{16}O, ^{40}Ca, ^{48}Ca, and ^{208}Pb nuclei within the random phase approximation (RPA) theory, finding that the description of low-lying magnetic states of doubly-closed-shell nuclei imposes severe constraints on the spin and tensor terms of the nucleon-nucleon effective interaction. We first used four phenomenological effective interactions, and we obtained good agreement with the experimental magnetic spectra and, to a lesser extent, with the electron scattering responses. Then we made self-consistent RPA calculations to test the validity of the finite-range Gogny D1 interaction. For all the nuclei under study, we found that this interaction inverts the energies of all the magnetic states forming isospin doublets.

DOI: 10.1103/PhysRevC.79.044311 PACS number(s): 21.60.Jz, 21.10.Re, 21.30.Fe, 25.30.Dh

I. INTRODUCTION

In the last 30 years, electron scattering experiments on nuclei have produced an enormous amount of high-precision, accurate, and reliable data, which impose severe constraints on nuclear models and theories.

Our interest is focused on the excitation of unnatural parity states in the low-lying region of the nuclear spectrum, where many responses of several nuclei have been measured [1–10]. The description of these states with effective theories, such as the Random Phase Approximation (RPA), indicates a strong sensitivity to the details of the spin- and tensor-dependent terms of the nucleon-nucleon (NN) effective interactions. While the study of a single excited state, or of a limited set of excited states, for a single nucleus has been pursued in depth, as, for example, in Refs. [11–13], a systematic study of a large set of nuclei and excited states has not been presented, and the availability of many precise experimental data has not been fully exploited.

We present here results of such a systematic study, which indicate that there are general requirements that the NN effective interaction has to fulfill in order to provide a reasonable description of the low-lying magnetic excitations. We obtained these results by using a phenomenological approach to the RPA theory inspired by the Landau-Migdal (LM) theory of finite Fermi systems [14,15]. In this approach, the mean-field (MF) basis, which provides the set of single particle energies and wave functions to be used in the RPA calculations, is generated by a Woods-Saxon well, whose parameters are adjusted to reproduce at best some ground state properties of the nucleus, such as the charge density distribution and the single particle energies around the Fermi surface. In addition, a phenomenological residual NN effective interaction is used. The parameters of this interaction are chosen to reproduce the energy of some specific excited states. In terms of comparison with the experimental data, this phenomenological approach uses the RPA theory at its best.

To study the sensitivity of our results to the details of the residual interaction, we have developed four phenomenological interactions, two of them having a zero range, as in the original formulation of the Landau-Midgal theory, and the other two having a finite range. For each type of interaction, we have considered a parametrization that includes tensor terms and another one without them, and we used these interactions to study the excitation of the low-lying magnetic spectra of ^{12}C, ^{16}O, ^{40}Ca, ^{48}Ca, and ^{208}Pb nuclei. We have found only a few cases that are sensitive to the differences between the various interactions, and we present them in the paper. The main result of our study is, however, that most of the states are equally well described by all the interactions we have considered. This suggests that we have been able to include some general features of the interaction, which are necessary for the description of the magnetic excitation spectra of doubly-closed-shell nuclei.

To test this hypothesis, we then repeated our RPA calculations within a fully self-consistent approach. This means that the MF states and energies were obtained within the Hartree-Fock (HF) approximation, using the same NN effective interaction employed in the RPA calculations. In particular, we used the Gogny D1 finite-range interaction [16–18]. In this case, we found remarkable disagreement with the experimental data, the most striking result being that all the energies of the states forming an isospin doublet are inverted. This indicates that the good results obtained with the phenomenological approach are not accidental, and that the study of the magnetic spectra is selective in choosing the strength of the relevant terms of the force.

The paper is organized as follows. In Sec. II, we give some details of our calculations, mainly regarding the input used to solve the RPA equations. The results of our phenomenological study of several magnetic states for all the nuclei under investigation are presented in Sec. III. In Sec. IV, we give the results of the self-consistent calculation using the Gogny

D1 interaction, for some selected cases. Finally, in Sec. V, we draw our conclusions.

II. DETAILS OF THE CALCULATION

The first input required by the RPA calculation is the set of single-particle wave functions and energies. In the phenomenological calculations, we used the single-particle bases generated by Woods-Saxon wells. The parameters of the wells were taken from the literature [19] and chosen to best describe the energies of the single-particle states around the Fermi surface and the ground state charge density distributions. In the self-consistent calculations, the single-particle wave functions and energies were obtained by solving the HF equations with the method described in Refs. [20,21].

We solved the RPA equations by using a discrete set of single-particle wave functions and energies. In the phenomenological calculations, the discretization of the continuum was obtained by diagonalizing the Woods-Saxon well in a harmonic oscillator basis. In the self-consistent calculations, the discretization was obtained by imposing the correct boundary conditions of a bound state to the single-particle wave functions at the edge of the computing box. The global RPA solutions strongly depend on the size of the single-particle configuration space [22]. However, there are excited states dominated by particle-hole excitations where the particle wave function is bound. In this article, we consider only this type of state.

For each nucleus considered, we used single-particle configuration spaces large enough to ensure the stability of the results for the states under investigation. In the phenomenological calculation, the smallest configuration space, used for ^{12}C, is composed of five major harmonic oscillator shells, for a total of 44 single-particle states. The largest space was used for ^{208}Pb, and it is composed of nine major shells for protons and ten major shells for neutrons, for a total of 100 single-particle states. In the self-consistent calculations, we fixed the size of the computational box, $R_{\max}$, and the maximum energy of the particle states in the configuration space, $E_{\rm cut}$. In the case of ^{12}C, $R_{\max} = 10$ fm and $E_{\rm cut} = 50$ MeV; whereas for ^{208}Pb, these two parameters are 14 fm and 50 MeV, respectively.

The second input required by RPA is the residual interaction, which, as done for the microscopic NN interactions of Urbana or Argonne type, we write as

$$\begin{aligned} V_{\rm eff}(1,2) &= v_1(r_{12}) + v_1^{\rho}(r_{12})\rho^{\alpha}(r_1,r_2) \\ &\quad + \left[v_2(r_{12}) + v_2^{\rho}(r_{12})\rho^{\alpha}(r_1,r_2)\right]\boldsymbol{\tau}(1)\cdot\boldsymbol{\tau}(2) \\ &\quad + v_3(r_{12})\,\boldsymbol{\sigma}(1)\cdot\boldsymbol{\sigma}(2) + v_4(r_{12})\,\boldsymbol{\sigma}(1)\cdot\boldsymbol{\sigma}(2)\,\boldsymbol{\tau}(1)\cdot\boldsymbol{\tau}(2) \\ &\quad + v_5(r_{12})S_{12}(\hat{r}_{12}) + v_6(r_{12})S_{12}(\hat{r}_{12})\boldsymbol{\tau}(1)\cdot\boldsymbol{\tau}(2). \end{aligned} \tag{1}$$

Here, following the indications of past phenomenological [15] and self-consistent [17] RPA studies, we have included a possible dependence on the nuclear one-body density $\rho(r)$ in the central and isospin channels. In Eq. (1), $r_{12} = |\boldsymbol{r}_1 - \boldsymbol{r}_2|$, $\boldsymbol{\sigma}$ and $\boldsymbol{\tau}$ are the usual spin and isospin operators, S_{12} is the tensor operator defined as

$$S_{12}(\hat{r}) = 3\,\boldsymbol{\sigma}(1)\cdot\hat{r}\boldsymbol{\sigma}(2)\cdot\hat{r} - \boldsymbol{\sigma}(1)\cdot\boldsymbol{\sigma}(2), \tag{2}$$

and

$$\rho(r_1,r_2) = [\rho(r_1)\rho(r_2)]^{1/2}. \tag{3}$$

The $v_i(r)$ functions of Eq. (1) are the same for all nuclei under investigation. On the other hand, the $v_i^{\rho}(r)$ corresponding to the density-dependent part of the interaction are assumed to be different for each nucleus: they were chosen to reproduce the first 2^+ state in ^{12}C and the first 3^- state in ^{16}O, ^{40}Ca, and ^{208}Pb. The other terms of the force were chosen to obtain a reasonable description of the centroid energy of the isovector giant dipole resonance by caring that the isoscalar spurious 1^- excitation is at zero energy or below. These criteria are useful for the scalar and isospin terms which are the most important terms responsible for the excitation of natural parity states. The $v_i(r)$ functions of the spin, spin-isospin, and tensor channels of the interaction ($i = 3, 4, 5$, and 6) were adjusted to describe the excitation energies of the magnetic states below 8 MeV in ^{208}Pb, paying particular attention to the 1^+ states at 5.85 and 7.30 MeV [23], and to the 12^- states at 6.43 and 7.08 MeV [3]. In addition, we also took care that the correct sequence of the two 1^+ states in ^{12}C forming an isospin doublet [2] was obtained, and that the energy of the first 4^- state of ^{16}O [9] was reasonably reproduced.

In this work, we are interested in the possible effects of the tensor channels of the interaction as well as in the relevance of its range (zero or finite). Thus, we have built four interactions. In connection with previous RPA studies [11], we considered two interactions, based on the Landau-Migdal approach and labeled LM and LMtt in the following, which have zero range. For these two cases, the functions $v_i(r)$ of Eq. (1) are given by

$$v_i(r_{12}) = V_i\delta(\boldsymbol{r}_1 - \boldsymbol{r}_2), \quad i = 1,\ldots,6. \tag{4}$$

The values of the parameters V_i, in MeV fm^3, are $V_1 = -918$; $V_2 = 600$; $V_3 = 20$; $V_4 = 200$; and $V_5 = 0$. For the LM interaction, $V_6 = 0$, while for the LMtt one, $V_6 = -150$ MeV fm^3.

Also, the terms $v_i^{\rho}(r)$ of Eq. (1) have zero range, i.e.,

$$v_i^{\rho}(r_{12}) = V_i^{\rho}\delta(\boldsymbol{r}_1 - \boldsymbol{r}_2), \quad i = 1, 2. \tag{5}$$

In MeV fm^6 units, the values of V_1^{ρ} are 361.0, 436.4, 492.3, and 599.0 and those of V_2^{ρ} are -40.0, -31.0, -150.0, and 0.0 for the ^{12}C, ^{16}O, ^{40}Ca, and ^{208}Pb, respectively. For ^{48}Ca, we used the same values as for ^{40}Ca. In all the calculations within the phenomenological approach, we used $\alpha = 1$ in Eq. (1).

In our phenomenological RPA approach, we considered only the contribution of direct matrix elements, assuming that the effects of the exchange terms are effectively included in the choice of the parameters of the various interactions. Therefore, the scalar and isospin terms, v_1 and v_2, respectively, do not contribute to the excitation of unnatural parity states, which are the focus of this work. For sake of completeness, however, we present here the full effective interactions.

We also considered two finite-range interactions with and without the tensor terms, which we labeled FRtt and FR, respectively. They were obtained from the Argonne V18 potential [24], by modifying its short-range behavior to take into account short-range correlations effects. In particular,

TABLE I. Parameters of the Gaussian functions of the FR and FRtt interactions [see Eq. (6)]. The spin terms, $i = 3$, have been set to zero.

Channel	a_1^i (MeV)	b_1^i (fm^{-2})	R_1^i (fm)	a_2^i (MeV)	b_2^i (fm^{-2})	R_2^i (fm)
$i = 1$	600.0	4.0	0.5	−200.0	20.0	0.0
$i = 2$	300.0	7.0	0.5			
$i = 4$	−40.0	4.5	0.5			

the short-range part of the Argonne V18 NN potential is removed and replaced by a combination of Gaussian functions. Specifically, we took

$$v_i(r) = \widetilde{V}_{18}^i(r) + \sum_{\mu=1}^{M} a_\mu^i \exp\left[-b_\mu^i \left(r - R_\mu^i\right)^2\right], \quad i = 1, \ldots, 4, \tag{6}$$

where $\widetilde{V}_{18}^i(r)$ are the corresponding terms of the bare Argonne V18 potential with their short-range terms set to zero. In Eq. (6), M is the number of Gaussians used in each channel. For the scalar channel, we included two Gaussians to obtain an attractive behavior starting from the repulsive core. The repulsive behavior is accounted for by the density-dependent term. For the channels $i = 2$ and $i = 4$, we used only one Gaussian, and we set to zero the spin term $i = 3$. The values of the various parameters are given in Table I, and they are the same for both interactions.

In the FRtt case, the tensor channels were obtained by multiplying the bare V18 tensor terms by the scalar term of the two-body short-range correlation function $f(r)$ of Ref. [19], that is,

$$v_i(r) = V_{18}^i(r) f(r), \quad i = 5, 6. \tag{7}$$

More specifically, we used the correlation functions obtained with the so-called Euler procedure, and because of the small differences between the $f(r)$ of the various nuclei [19], we used the function obtained for ^{40}Ca in all our calculations. In the FR interaction, the tensor terms are equal to 0.

Finally, the density-dependent terms were taken to be Gaussians:

$$v_i^\rho(r) = A_i \exp(-B_i r^2), \quad i = 1, 2. \tag{8}$$

In our calculations, we used $B_i = 1$ fm^{-2}. The values of the parameter A_i are shown in Table II.

TABLE II. Parameters (in MeV) of the density-dependent terms of the FR and FRtt interactions [see Eq. (8)].

Nucleus	FR		FRtt	
	A_1	A_2	A_1	A_2
^{12}C	133.8	−120.0	133.8	−125.0
^{16}O	163.4	−95.0	163.6	−95.0
^{40}Ca	194.7	−50.0	194.6	−50.0
^{208}Pb	240.0	−25.0	240.0	−25.0

The free parameters of the finite-range interactions were chosen following the same criteria used for the zero-range interactions, and also in this case we included in the RPA calculations only the contributions of the direct terms of the matrix elements.

In our self-consistent RPA calculations, we employed a Gogny interaction [16–18], which is usually expressed as

$$\begin{aligned} V_{\rm eff}(1,2) = &\sum_{i=1}^{2} \exp\left[-\frac{(\boldsymbol{r}_1 - \boldsymbol{r}_2)^2}{\mu_i^2}\right] \\ &\times (W_i + B_i \hat{P}_\sigma - H_i \hat{P}_\tau - M_i \hat{P}_\sigma \hat{P}_\tau) \\ &+ W_{LS}(\boldsymbol{\sigma}(1) + \boldsymbol{\sigma}(2)) \overleftarrow{k} \times \delta(\boldsymbol{r}_1 - \boldsymbol{r}_2) \vec{k} \\ &+ t_0(1 + x_0 \hat{P}_\sigma)\delta(\boldsymbol{r}_1 - \boldsymbol{r}_2)\rho^\alpha\left(\frac{1}{2}(\boldsymbol{r}_1 + \boldsymbol{r}_2)\right), \end{aligned} \tag{9}$$

where $\vec{k}$ is the operator of the relative momentum

$$\vec{k} = \frac{1}{2i}(\nabla_1 - \nabla_2). \tag{10}$$

We have indicated with $\hat{P}_\sigma$ and $\hat{P}_\tau$ the usual spin and isospin exchange operators, and μ_i, W_i, B_i, H_i, M_i, W_{LS}, t_0, and x_0 are constant parameters.

The relation between the expression above of the Gogny force and that required by Eq. (1) is obtained from the following equations:

$$v_1(r) = W(r) + \frac{B(r)}{2} - \frac{H(r)}{2} - \frac{M(r)}{4}, \tag{11}$$

$$v_2(r) = \frac{B(r)}{2} - \frac{M(r)}{4}, \tag{12}$$

$$v_3(r) = -\frac{H(r)}{2} - \frac{M(r)}{4}, \tag{13}$$

$$v_4(r) = -\frac{M(r)}{4}, \tag{14}$$

where

$$F(r) = \sum_{i=1}^{2} F_i \exp\left(-\frac{r^2}{\mu_i^2}\right), \quad F \equiv W, B, H, M. \tag{15}$$

The density-dependent term of Eq. (9) can be written as

$$t_0(1 + x_0 \hat{P}_\sigma)\rho^\alpha = \left[t_0\left(1 - \frac{x_0}{2}\right) - \frac{t_0 x_0}{2}\boldsymbol{\tau}(1)\cdot\boldsymbol{\tau}(2)\right]\rho^\alpha. \tag{16}$$

In particular, we used the parametrization of the Gogny interaction known as D1 [16–18]. In the HF calculations, we included all the terms of the interactions; whereas in the RPA calculations, we neglected the contribution of the spin-orbit term. In HF and RPA calculations, both direct and exchange terms of the interaction matrix elements were considered.

The various interactions used in our work are shown in Fig. 1 as a function of the relative momentum of the interacting pair of nucleons. In this figure, solid, dashed, and dotted lines represent the D1, LMtt, and FRtt interactions, respectively. Our tensor-dependent interactions were obtained by adding the two tensor-dependent terms $v_{5,6}(r)$ to the LM and FR four central channels. For this reason, in the figure, the LM and

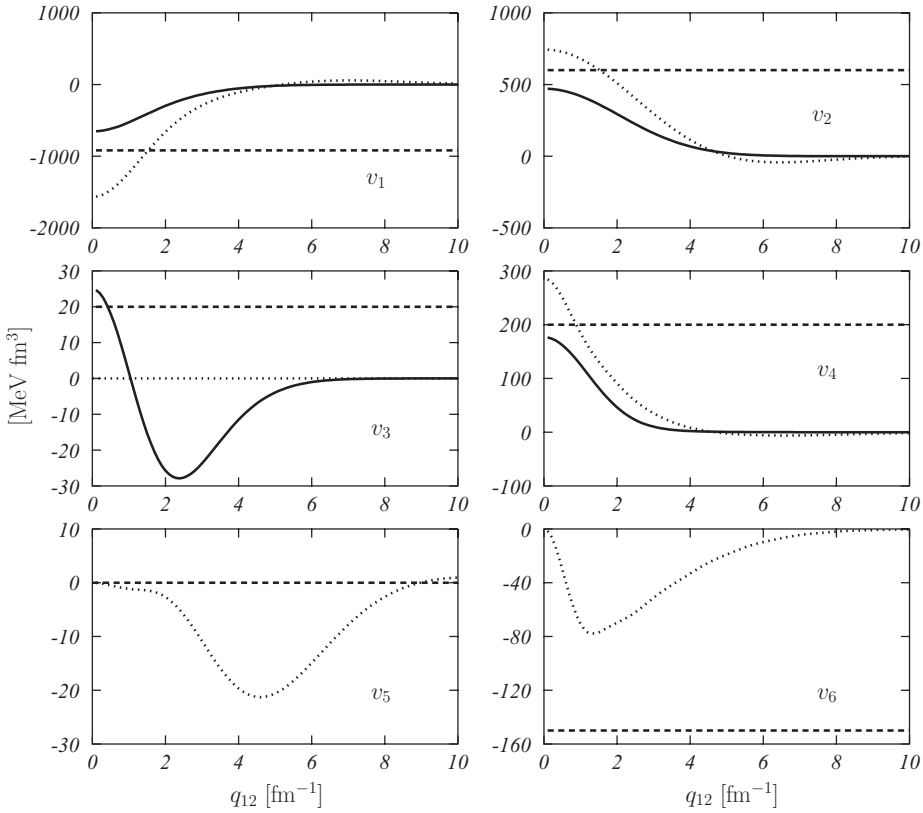

FIG. 1. Effective NN interactions used in this work as a function of the relative momentum. The solid lines represent the D1, dashed lines the LMtt, and dotted lines the FRtt interactions. The central channels $v_1 \ldots v_4$ of LMtt and FRtt interactions are identical to those of the LM and FR interactions, respectively.

FR interactions are not shown, since they are identical, in the central channels, to the LMtt and FRtt interactions. The zero-range interaction terms are constant in momentum space. We point out that the spin term v_3 was set to zero in the FR and FRtt interactions, and that LMtt does not have the pure tensor term v_5. The finite-range interactions FR, FRtt, and D1 have similar asymptotic behavior above 4 fm^{-1}. The values of the LM and LMtt interactions fall between those of the D1, FR, and FRtt interactions at $q_{12} \sim 0$.

When a discrete configuration space of single-particle wave functions is used, the solution of the RPA equations is obtained by solving a homogeneous system of linear equations. For a given excitation multipole of angular momentum J and parity π, the RPA solution, obtained with standard diagonalization procedures, provides the set of excitation energies, and, for each excited state, the full set of RPA amplitudes $X^{J^\pi}_{\text{p-h}}$ and $Y^{J^\pi}_{\text{p-h}}$. One can then calculate the amplitudes for the transition between ground and excited states induced by an operator $T_J(q)$ as

$$\langle J\|T_J(q)\|0\rangle = \sum_{\text{ph}} \left[X^{J^\pi}_{\text{ph}} \langle j_p\|T_J(q)\|j_h\rangle + (-1)^{J+j_p-j_h} \times Y^{J^\pi}_{\text{ph}} \langle j_h\|T_J(q)\|j_p\rangle\right]. \quad (17)$$

In the equation above, $|j\rangle$ indicates the single-particle wave function characterized by the set of quantum numbers including the principal quantum number, orbital angular momentum, total angular momentum j, and isospin third component. The double bars indicate the reduced matrix elements of the angular coordinates.

In this work, we calculated electromagnetic responses, which are defined as the Fourier transform of the squared moduli of the transition amplitude (17) [1]. In the plane-wave Born approximation description of inelastic electron scattering experiments, these responses, which depend on the modulus of the momentum transfer q, are related to the cross section by multiplicative factors depending on kinematics variables, and to the Mott cross section [25,26].

Since we are interested in magnetic states, the charge operator does not contribute. The operators we used to calculate the transition amplitudes (17) are those of the convection and magnetization currents. The explicit expressions of the single-particle matrix element can be found in Refs. [27,28]. We did not consider the contribution of meson-exchange currents, which, for low-lying excited states, has been found to be negligible in comparison with the effects of the residual interaction [11,29].

III. RESULTS OF THE PHENOMENOLOGICAL APPROACH

In this section, we present our results for the low-lying magnetic states of ^{12}C, ^{16}O, ^{40}Ca, ^{48}Ca, and ^{208}Pb, obtained within the phenomenological approach. For each nucleus, we first present the unnatural parity low-energy spectrum, we compare it with the measured spectrum, and we discuss the sensitivity of the excitation energies to the inclusion of finite-range and tensor term contributions in the residual interaction. Then, for some specific states, we investigate the electromagnetic transverse response functions. To minimize

the uncertainties due to the discretization of the continuum, we select excited states that are dominated by particle-hole (p-h) pairs in which the particle is in a bound state. Furthermore, we choose the states that exhibit the largest sensitivity to those terms of the residual interaction that are the focus of the present study. Also, we address our attention to those states forming isospin doublets, because their structure (order of the states and relative splitting) is sensitive to the isospin-dependent terms of the residual interactions and, more specifically, to the tensor-isospin terms we introduced in the previous section. The interest in isospin doublets will become clearer in connection with the self-consistent calculations, which will be presented in the next section. In addition, we give preference to the study of those states for which experimental data are available.

A detailed discussion of the results will be presented throughout this section, but we would like to anticipate that we have obtained a general good description of the excitation spectra, almost independently of the effective interaction used. This indicates that we have been able to incorporate in the parametrization of the residual interaction some relevant features required by the description of the magnetic excitations. The disagreement with the experimental data can be due to the use of the plane-wave Born approximation in the calculation of the electron scattering cross section, or in the nuclear structure part, to the truncation of the configuration space. Actually these approximations are rather well controlled. The experimental responses are usually presented after a correction for the Coulomb distortion of the electron wave functions, and the effects of the limited configuration space are effectively considered by the choice of the force parameters. For these reasons, we think that the possible discrepancies between our predictions and the experimental data have to be ascribed more to the intrinsic limitations of the RPA theory than to a more efficient parametrization of the interaction.

A. The ^{12}C nucleus

In Table III, we compare the energies of the low-lying magnetic states of ^{12}C with the experimental values taken from Ref. [30]. In the calculation with the LM interaction, we are unable to identify the second 2^- state, because all the states higher than the first one have dominant p-h components with the particle in the continuum. Apart from this case, we notice that the calculated energies for each state are rather similar, independent of the interaction used. The experimental energies are reasonably well reproduced except for the 2^- states whose energies are about 4 MeV above the experimental ones.

TABLE III. Low-lying spectrum of the unnatural parity, magnetic, states in ^{12}C. The energies are expressed in MeV. The experimental values are from Ref. [30].

	^{12}C				
J^π	LM	LMtt	FR	FRtt	Exp
2^-	16.26	16.20	16.07	16.03	11.83
1^+	14.41	14.41	13.89	13.87	12.71
2^-	–	17.26	17.23	17.14	13.35
1^+	18.13	17.97	18.17	18.05	15.11
4^-	18.21	18.21	17.78	17.75	18.27
4^-	21.70	20.80	19.92	19.49	19.50

The two most interesting cases are the 1^+ and 4^- states. For the 1^+ case, we obtain two states, dominated by the $[(1p_{1/2})(1p_{3/2})^{-1}]$ proton and neutron pairs, although for the state with higher energy non-negligible contributions of other p-h pairs appear. The lowest energy state has an isoscalar (IS) character, while the state with higher energy is isovector (IV). These states correspond to the experimentally well-known isospin doublet at 12.71 MeV ($T = 0$) and 15.11 MeV ($T = 1$) [8,30]. The corresponding transverse response functions, or form factors, are shown as a function of the effective momentum transfer in the upper panels of Fig. 2. We use the traditional definition of the effective momentum [1]

$$q_{\text{eff}} = q\left(1 + \frac{3Z\alpha\hbar c}{2\epsilon_i R}\right), \tag{18}$$

where Z is the atomic number of the target nucleus, α is the fine structure constant, ϵ_i is the incident electron energy, and R is the nuclear charge radius.

In the lower panels of the same figure, for each state considered, we show the proton (thick lines) and neutron (thin lines) contributions to the transition densities, as a function of the distance from the center of the nucleus. These transition densities were obtained from Eq. (17) by considering for T_J the expression of the magnetization and avoiding the integration on r. The behavior of the transition densities clearly shows the isospin nature of the two states. For the lower energy state, proton and neutron densities are in phase, indicating the IS nature of the excitation. The opposite happens for the second state, and this is a clear signature of the IV nature of this state.

As we can see from Table III, our calculations overestimate the experimental energies of both the 1^+ states and their splitting. The largest relative differences in the energy values are 13% and 20% for the first and second state, respectively. Despite these quantitative discrepancies with the observed energies, our calculations produce the correct sequence of isoscalar and isovector excitation with all the interactions. The inclusion of finite-range and tensor terms changes the energy values at the level of few percent. Also the response functions are not very sensitive to the use of different residual interactions, as shown in Fig. 2. Only the responses of the IV state show some difference around the minimum at $q_{\text{eff}} = 1.5$ fm^{-1}. The position of this minimum seems to be slightly better described by the interactions including tensor terms. The comparison with electron scattering data [9] shows good agreement with the IS data and overestimates the experimental IV response in the region of the first maximum. A good description of the 1^+ IV transition is extremely important, since this state is used in liquid scintillator neutrino detectors to identify neutral current events [31]. The figure shows that the discrepancy in the description of the IV response cannot be solved by using an overall quenching factor. While the first peak is overestimated by almost a factor of 2, the second peak is rather well reproduced. The difficulty in describing the IV 1^+ state is a common characteristic of the RPA calculations [32–36] and produces an overestimation of the experimental total neutrino ^{12}C cross sections measured in

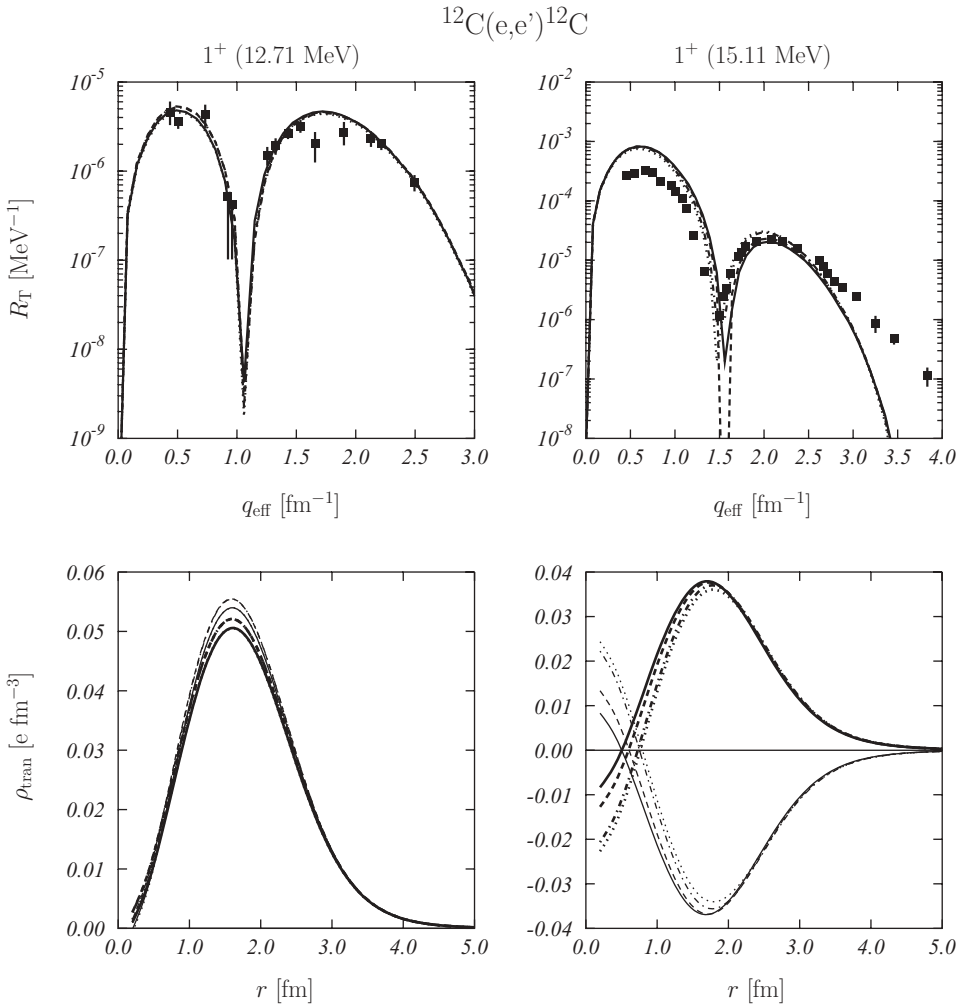

FIG. 2. Upper panels show the electromagnetic responses of the 1^+ states in ^{12}C. The data are from Ref. [9]. The various lines indicate the interaction used in the RPA calculation: LM (solid), LMtt (dotted), FR (dashed), and FRtt (dashed-dotted). The lower panels show proton (thick lines) and neutron (thin lines) contributions to the transition densities of the two states. The line types have the same meaning as in the upper panels. The values of the experimental energies for the two states are indicated.

the LNSD [31,37,38] and KARMEN [39] experiments. To solve the problem, the presence of strong pairing effects has been advocated [40], with the idea that the shell closure in the ^{12}C nucleus is not a good approximation. We have to remark, however, that the problem of describing the IV 1^+ state is present also in other doubly-magic nuclei where pairing correlations are negligible [23]. The size of the first maximum of the 1^+ IV response in ^{12}C is well reproduced by microscopic *ab initio* shell model calculations [41], but the shape is completely wrong. These calculations produce the first minimum of the response at 2 fm^{-1}, and they are completely missing both size and shape of the second maximum.

We consider now the 4^- states which also form an isospin doublet. These states are dominated by the linear combination of the stretched $[(1d_{5/2})(1p_{3/2})^{-1}]$ excitations. In our calculations, the $1d_{5/2}$ state is bound with an energy of -1.1 MeV in the neutron case, and it shows a sharp resonance at 2.0 MeV in the case of protons. The MF excitation energies are the single-particle energy differences, which for this p-h transitions are 17.96 and 17.62 MeV for protons and neutrons, respectively. The RPA calculations mix the proton and neutron p-h transitions, and in our results the isoscalar state has lower energy than the isovector one, independent of the interaction used. The results shown in Table III indicate that the residual interaction produces solutions with energies higher than those obtained within the simple MF. In this situation, the role of the finite range of the force is not negligible. The upward shift of the RPA solutions is reduced by only 0.5 MeV for the IS state, but by 1.7 MeV for the IV state. The experimental IS energy is better reproduced by the zero-range interaction, while the IV energy is much better described by the FRtt interaction.

We show in Fig. 3, the electromagnetic responses for the two 4^- states. We compare the IV responses to the available experimental data [4]. The IS responses show some sensitivity to the use of the residual interaction. The inclusion of the tensor terms and the finite range reduces the size of the response. The results of the IV responses are rather independent of the residual interaction, and the experimental data are rather well reproduced.

Finally we observe that our model also produces 2^- states, however, as said before, their energies are in large disagreement with data. The same occurs when the corresponding responses are compared. This might be due to the presence, in these states, of sizable contributions from p-h pairs having a particle in the continuum, which brings in further uncertainties, as our procedure discretizes the continuum.

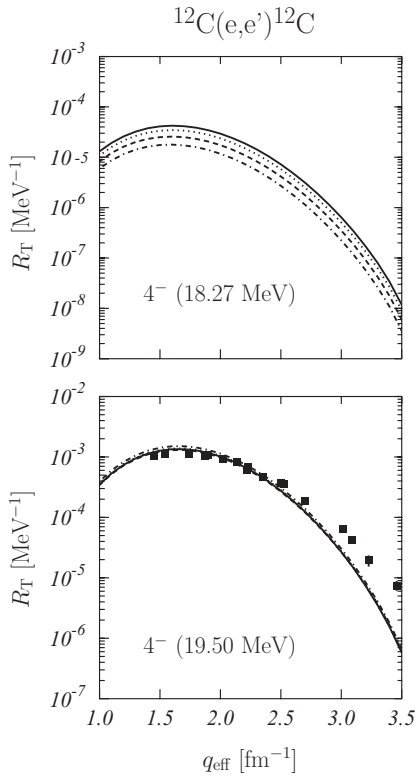

FIG. 3. Electromagnetic responses of the 4^- states in ^{12}C. The meaning of the lines is the same as in Fig. 2. The data are from Ref. [4].

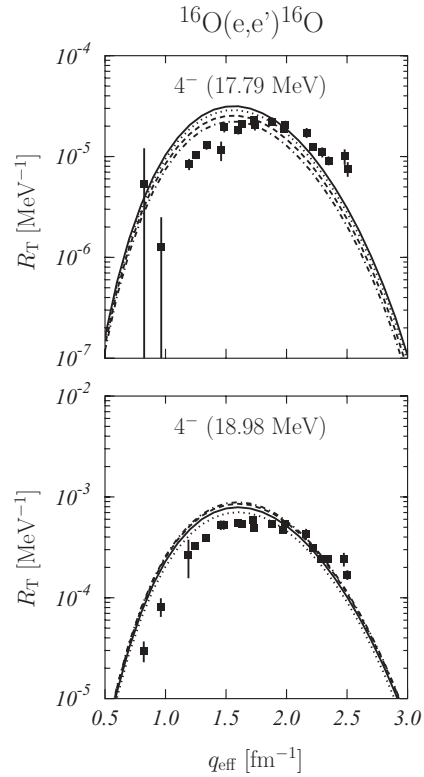

FIG. 4. Same as Fig. 3, but for ^{16}O. The data are from Ref. [9].

B. The ^{16}O nucleus

The spectrum of the low-lying magnetic states obtained with the four interactions is presented in Table IV, where it is compared with the experimental spectrum [30]. All the states have negative parity and, since the p shell is closed for both protons and neutrons, this indicates that they are dominated by p-h transitions involving neighbor shells. The order of the various states is reproduced by our calculations. The magnetic state with lowest energy is a 2^- state, as in the experimental spectrum, but the calculated energy eigenvalues overestimate the experimental value by about 30%, independent of the interaction used. This result is contrary to our expectations, because this state is dominated by the $[(1d_{5/2})(1p_{1/2})^{-1}]$ bound proton and neutron transitions, and therefore it should be well described by our approach. We have found [22] a remarkable disagreement with the experimental data [9] also for the transition density. These facts indicate the presence, in this 2^- state, of effects beyond the description capability of our RPA model.

TABLE IV. Same as in Table III, but for ^{16}O.

	^{16}O				
J^π	LM	LMtt	FR	FRtt	Exp
2^-	11.80	11.80	11.51	11.51	8.87
0^-	12.33	11.19	12.15	11.84	10.96
0^-	–	12.39	13.13	12.23	12.80
4^-	18.15	18.15	17.75	17.73	17.79
4^-	21.41	20.59	19.88	19.45	18.98

The subsequent states in our spectrum are two 0^- states which can be identified in the experimental spectrum [30]. They are dominated by the $[(2s_{1/2})(1p_{1/2})^{-1}]$ proton and neutron transitions. The effect of the tensor term of the interaction on the energy values is not negligible. Since these states are not excited by electromagnetic probes, at least in the one-photon exchange picture, we calculated the neutrino and antineutrino cross sections [22] and we found large sensitivity to the tensor force. This point deserves a more detailed investigation, for example, by calculating the excitations induced by hadronic probes.

The 4^- states, dominated by $[(1d_{5/2})(1p_{3/2})^{-1}]$ protons and neutrons p-h excitations, form an isospin doublet. Also in this case, the energy of the IS state is lower than that of the IV one, in agreement with the experimental data. The IS energy eigenvalues are almost insensitive to the presence of tensor terms; they are, however, rather sensitive to the use of finite-range interactions. In the IV case, both tensor terms and the finite range affect the energy value. The electromagnetic responses for the two states are shown in Fig. 4 and compared with the experimental data of Ref. [9]. In both cases, the position of the maximum of our calculations is slightly lower than the experimental one. The IS state shows some sensitivity to the residual interaction. The inclusion of the tensor term and the finite range contributes to lowering the response, and this slightly improves the comparison with the data. The IV

TABLE V. Same as in Table III, but for ^{40}Ca.

^{40}Ca					
J^π	LM	LMtt	FR	FRtt	Exp
4^-	6.86	6.88	6.78	6.80	5.61
2^-	7.21	7.20	6.91	6.90	7.53
4^-	7.52	7.59	7.42	7.47	7.66
2^-	8.90	8.44	8.76	8.58	8.42

response is less sensitive to the changes of the interaction. We obtain a general good agreement with the data.

C. The ^{40}Ca nucleus

The spectrum of the magnetic states of the ^{40}Ca nucleus is given in Table V. The global closure of the *s*-*d* shell, for both protons and neutrons, implies that the low-energy spectrum is composed only of negative-parity states. Our RPA calculations reproduce the correct sequence of the states, independent of the interaction used. The energy eigenvalues do not show large sensitivity to the choice of the interaction. We overestimate the energy of the first 4^- state, while the energies of the other states are better reproduced.

The response functions of the 2^- and 4^- states are shown in Fig. 5 and compared with the available experimental data [42]. The response of the lowest 2^- state is almost insensitive to the choice of the residual interaction. The electromagnetic response of the other 2^- state shows larger sensitivity to the interaction used in the RPA calculation. The shapes of the responses are strongly modified by the finite-range and especially by the tensor term. The latter lowers the value of the first maximum and reduces the width of the second peak of the response. The data are not accurate enough to allow a selection among the various results.

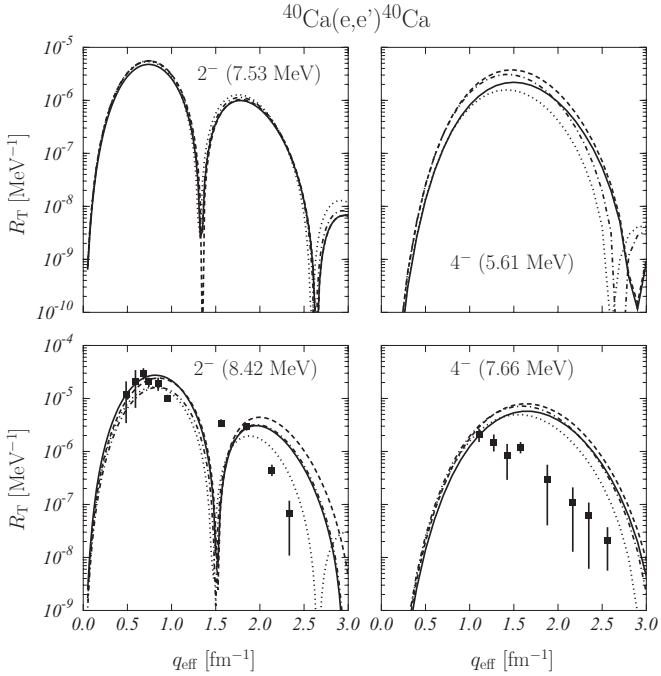

FIG. 5. Same as Fig. 3, but for the 2^- and 4^- states in ^{40}Ca. The data are from Ref. [42].

The response of the lowest 4^- state indicates that the presence of the finite-range increases the peak value, while the tensor term reduces it. The same effect is present also in the response of the other 4^- state. In this case, experimental data are available for comparison [42], and we see that there is no similarity in size and shape between our results and the data.

D. The ^{48}Ca nucleus

In Table VI, we present the low-energy magnetic spectrum of ^{48}Ca, obtained with the same residual interactions used for ^{40}Ca. The ^{48}Ca spectrum contains both negative- and positive-parity states, the latter being dominated by single-particle excitations of the $1f_{7/2}$ neutron-hole. Globally, we obtain a reasonable agreement between the measured and calculated energies, but the correct sequence of the excited states is not exactly reproduced. In each calculation, we obtain a 6^- state whose energy is larger than that of the 1^+ state, while experimentally the opposite occurs. This disagreement is due to the overestimation of the 6^- state energy by about 2.5 MeV. The energy eigenvalues presented in Table VI do not show particular sensitivity to the different interactions used in the RPA calculations.

The study of the electromagnetic responses of these states is more interesting, as shown in Fig. 6, where the theoretical curves are compared with the available experimental data [6, 43]. Large effects of the choice of the residual interaction are present for the 2^- and 6^- states. The residual interaction produces some differences also in the responses relative to the 4^-, 1^+, and 3^+ states.

As already mentioned, the positive-parity states are dominated by the excitation of the $1f_{7/2}$ neutron-hole, therefore the residual interaction plays a minor role, and the results are rather similar to those of the MF. Effects of the use of different interactions are present only at the third maximum of the 1^+ responses and at the first two maxima for the 3^+ state. The experimental data of the 3^+ and 5^+ are rather well reproduced. The same does not occur with the 1^+ state, where other mechanisms beyond RPA (second-order core polarization, tensor correlations, and Δ excitations) must be

TABLE VI. Same as in Table III, but for ^{48}Ca.

^{48}Ca					
J^π	LM	LMtt	FR	FRtt	Exp
3^+	5.03	4.99	4.96	4.94	4.61
5^+	5.26	5.16	5.04	4.98	5.15
4^-	6.44	6.41	6.36	6.35	6.10
2^-	7.53	7.06	7.30	7.10	6.89
6^-	11.29	11.31	11.01	10.99	8.56
1^+	9.65	9.38	9.68	9.50	10.23

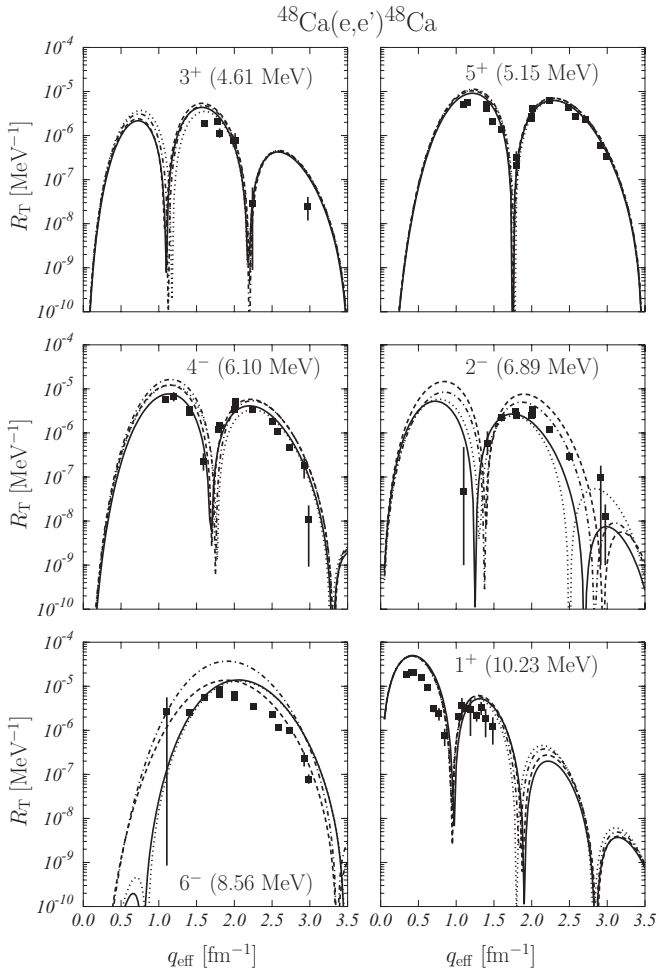

FIG. 6. Same as Fig. 3, but for the magnetic states in ^{48}Ca. The data are from Refs. [6,43].

taken into account to obtain good agreement between theory and experiment [44].

For the negative-parity states, we cannot find any common trend related to the inclusion of the various ingredients of the interactions. For example, the tensor term increases the responses of the 4^- and 6^- states, while it lowers that of the 2^- state. The 2^- and 4^- experimental responses are rather well reproduced. Similar results were obtained in Ref. [45], where the Jülich-Stony Brook interaction [46] with the tensor terms reduced by ∼30–60% was used. We have encountered problems in the description of the 6^- response. On the other hand, we have already pointed out the difficulties found in describing the excitation energy of this state.

E. The ^{208}Pb nucleus

The energies of the low-lying magnetic states of ^{208}Pb are presented in Table VII and compared with the experimental ones. The sequence of the states is quite well reproduced. There are some exceptions, but these occur with energy differences of the order of a few tens of keV, an energy resolution smaller than the accuracy we assign to our results. The global

TABLE VII. Same as in Table III, but for ^{208}Pb.

	^{208}Pb				
J^π	LM	LMtt	FR	FRtt	Exp
4^-	3.52	3.50	3.50	3.49	3.48
6^-	4.04	4.04	4.03	4.03	3.92
2^-	4.30	4.21	4.23	4.20	4.23
9^+	5.14	5.11	5.11	5.09	5.01
9^+	5.45	5.45	5.44	5.44	5.26
0^-	5.64	5.38	5.54	5.42	5.28
11^+	5.25	5.20	5.14	5.12	5.29
1^+	5.92	5.89	5.72	5.70	5.85
11^+	5.88	5.89	5.86	5.87	5.86
10^-	6.64	6.56	6.57	6.53	6.28
12^-	6.66	6.61	6.57	6.54	6.43
14^-	6.99	6.84	6.66	6.59	6.74
10^-	7.44	7.22	7.32	7.23	6.88
12^-	7.72	7.55	7.41	7.32	7.08
1^+	7.38	6.77	7.64	7.48	7.30

picture emerging from Table VII is that the various interactions produce small differences in the energy eigenvalues.

The investigation of the electromagnetic responses provides more information. We start our discussion with the 12^- responses, which have been studied quite often in the past [11,47,48] because of their apparently simple p-h structure. They are, in fact, mainly composed by two p-h pairs, the proton $[(1i_{13/2})(1h_{11/2})^{-1}]$ and neutron $[(1j_{15/2})(1i_{13/2})^{-1}]$ transitions. The lower 12^- state, experimentally found at 6.43 MeV, is neutron dominated; while the state at higher energy, 7.08 MeV, is dominated by the proton transition. Our calculations produce the correct order of the states, and the RPA energies agree well with the experimental values, especially the lower one. We must recall, however, that this state is one of the states used to set the values of the interaction parameters. The calculated energies of the higher state overestimate the experimental value, but the discrepancies are below 10%. The electromagnetic responses are shown in the right panels of Fig. 7 and are compared with the data of Ref. [3]. The responses relative to the higher state, lower right panel, show a reasonable agreement with the data, and they are almost insensitive to the choice of the residual interaction. On the contrary, the responses of the neutronic state, upper right panel, are extremely sensitive to the inclusion of both the finite range and tensor terms in the interaction. These effects improve the agreement with the data, but the calculated curves still underestimate the measured response. The disagreement could be reduced by increasing the magnitude of the tensor part of the interaction. We have found, however, that this would produce a general worsening of the magnetic spectrum of ^{208}Pb and of the other nuclei we have considered. For example, a too strong tensor interaction could invert the sequence of the IS and IV 1^+ states.

In the left panels of Fig. 7, we present the responses of the 10^- states, which show some sensitivity to the tensor part of the residual interaction. All interactions can reproduce the magnitude of the responses, but only the inclusion of the tensor

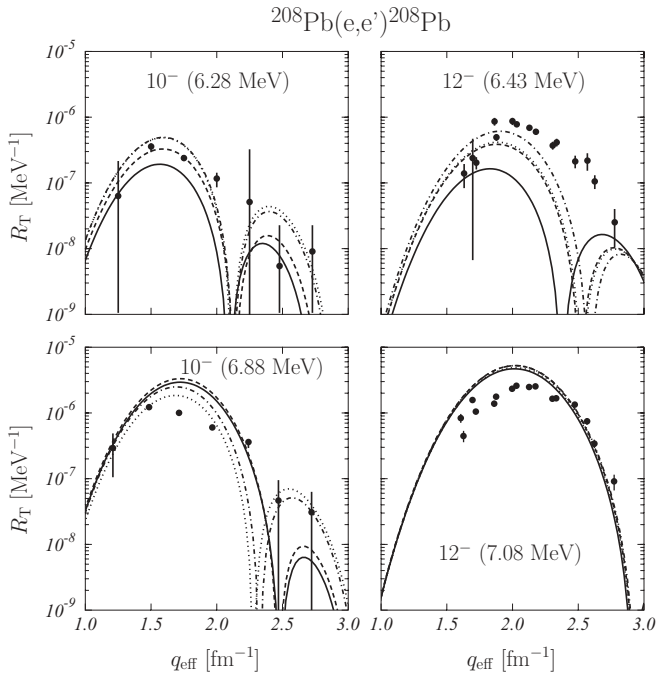

FIG. 7. Same as Fig. 3, but for the 10^- and 12^- states in ^{208}Pb. The data are from Ref. [3].

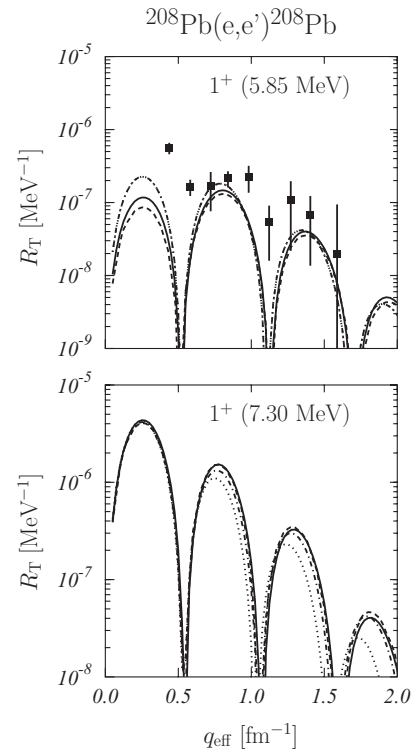

FIG. 8. Same as Fig. 3, but for the 1^+ states in ^{208}Pb. The data are from Ref. [5].

terms allows a good description of the second peak in both 10^- states. Improvements in the precision of experimental data around $q = 2.5$ fm^{-1} would thus be particularly important to studying the tensor component of the residual interaction.

The energies of the 1^+ states are reproduced rather well with all the residual interactions, except for the isoscalar state at 5.85 MeV and for the isovector state at 7.30 MeV. We should point out that the IV state is so fragmented that this energy value is an estimate based on an accurate analysis of the photon scattering data [23]. The electromagnetic responses are plotted in Fig. 8, and for the IS state (upper panel) we compare them with the data [5]. For this state, all the curves reproduce the q dependence of the data except at low q, where the theoretical responses are well below the data. Unfortunately there are no data in the region $q < 0.5$ fm^{-1} where the effects of the different interactions are larger. In the IV case (lower panel), the differences between the various results appear at large q values. This is, however, a theoretical speculation, because, as we have already said, experimentally the IV state is extremely fragmented and cannot be described within our RPA approach. In the ^{208}Pb nucleus, pairing effects are negligible, and we think that this fragmentation can be described only by considering elementary excitations beyond 1p-1h.

The 9^+, 11^+, and 14^- states are dominated by a single particle-hole excitation, with the exception of the lower energy 9^+ state, where a small contribution of the proton $[(2f_{7/2})(1h_{11/2})^{-1}]$ transition is present besides the dominant neutron $[(2g_{9/2})(1i_{13/2})^{-1}]$ one. For this state, the calculated transverse responses, presented in the upper left panel of Fig. 9, show three peaks, and this behavior is compatible with the data. On the other hand, the position of the experimental points of the other 9^+ state (lower left panel) is very different from the shape of the theoretical responses, which exhibit some dependence on the residual interaction. Analogous problems are found for the 11^+ states, whose responses are plotted in the right panels of Fig. 9.

To complete our survey, we show in Fig. 10 the electromagnetic response of the 14^- state. Its nature of almost pure p-h transition is evident, because there is no dependence on the residual interaction, as pointed out in the literature (see, for example, Ref. [49]).

IV. RESULTS OF SELF-CONSISTENT CALCULATIONS

In the previous section, we have presented the results of the phenomenological approach. We would like to point out that the study of the full set of magnetic states, together with their electromagnetic responses, can be used to test the validity of the effective interactions used in RPA calculations. To give an example of this potentiality, we present here some selected results we have obtained with the Gogny D1 interaction [16–18].

The complete D1 interaction was used in computing the HF single-particle energies and wave functions, while we neglected the contribution of the spin-orbit term in the RPA calculations. This is a good approximation if the contribution of the residual Coulomb interaction is also neglected [50], as we have done. The RPA results presented in this section were obtained by considering both direct and exchange terms of the D1 interaction, similar to what we did in the HF calculations. This makes the connection between the properties of the excitation spectrum and the various parts of the interaction much more complicated than in the phenomenological approach,

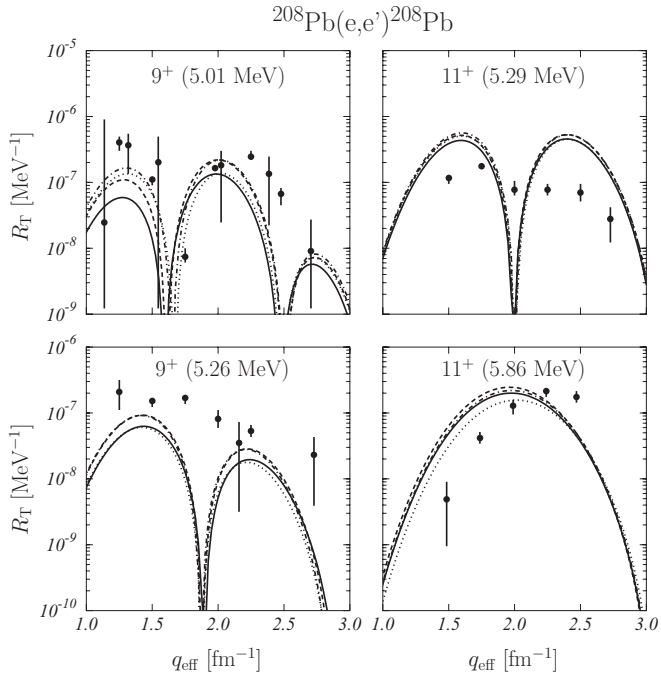

FIG. 9. Same as Fig. 3, but for the 9^+ and 11^+ states in ^{208}Pb. The data are from Ref. [3].

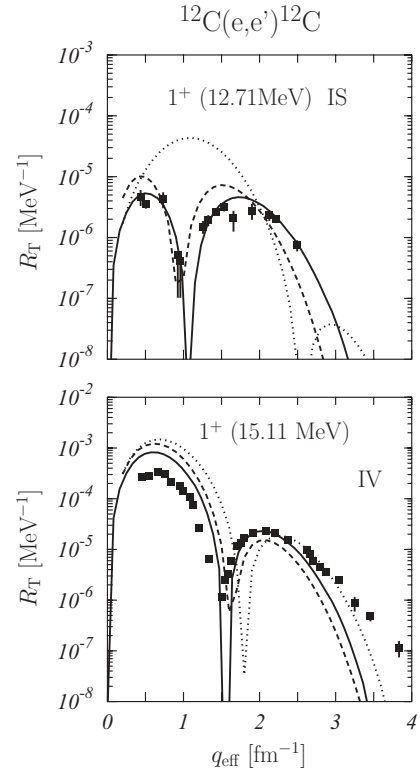

FIG. 11. Electromagnetic responses of the 1^+ isospin doublet in ^{12}C. The full lines show the results of Fig. 2 obtained with the FR interaction. The dotted lines were obtained with the D1 interaction but using the set of single-particle wave functions and energies used in the phenomenological approach. The dashed lines are the results of a self-consistent calculation with the D1 interaction. This means that the single-particle basis was generated by a HF calculation with the D1 interaction. The dotted and dashed curves in the IS panel were obtained by using the RPA amplitudes of the higher energy 1^+ solution. The lower energy amplitudes were used to generate the curves shown in the IV panel.

where only direct matrix elements were considered, because each interaction term can now contribute to the other channels through the exchange diagrams. For example, in the phenomenological case, scalar and isospin channels do not contribute to the excitation of unnatural parity states, whereas these two channels produce a contribution to the spin and spin-isospin channels in the exchange diagrams in the calculations done with the D1 interaction.

To complete the information about our RPA calculations, we point out that we have also included the so-called rearrangement terms, related to the density-dependent part of the interaction. They arise by considering the effective interaction as the second derivative of the energy with respect to the single-particle density [51]. Quantitatively, we found the contributions of these terms to be negligible in all the cases we investigated.

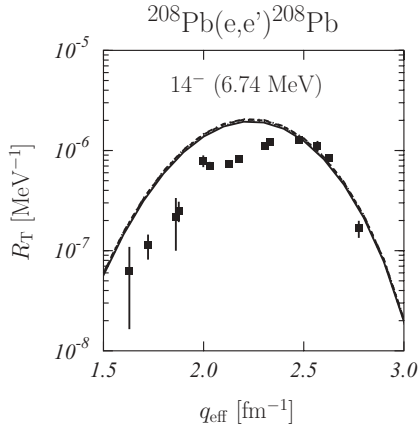

FIG. 10. Same as Fig. 3, but for the 14^- states in ^{208}Pb. The data are from Ref. [3].

In the following, we present two different types of results. In the first case, the Gogny D1 interaction is used in the RPA calculations, but the size of the configuration space and the single-particle wave functions and energies are taken to be the same as in the phenomenological approach. The results of these calculations are represented by the dotted lines in Figs. 11–13. The second case is fully self-consistent, i.e., the single-particle basis is produced by a HF calculation with the same interaction used in RPA. The size of the configuration space is chosen as described in Sec. II. The corresponding results are shown in the figures as dashed lines. The comparison between these two cases allows us to distinguish between the role played by the single-particle basis and that played by the residual interaction. In the figures, the full lines show the results obtained in the phenomenological approach by using the FR interaction. This interaction has a finite range, but it does not include the tensor terms; therefore, among the four interactions we have defined in the previous section, it is the most similar to the D1 interaction.

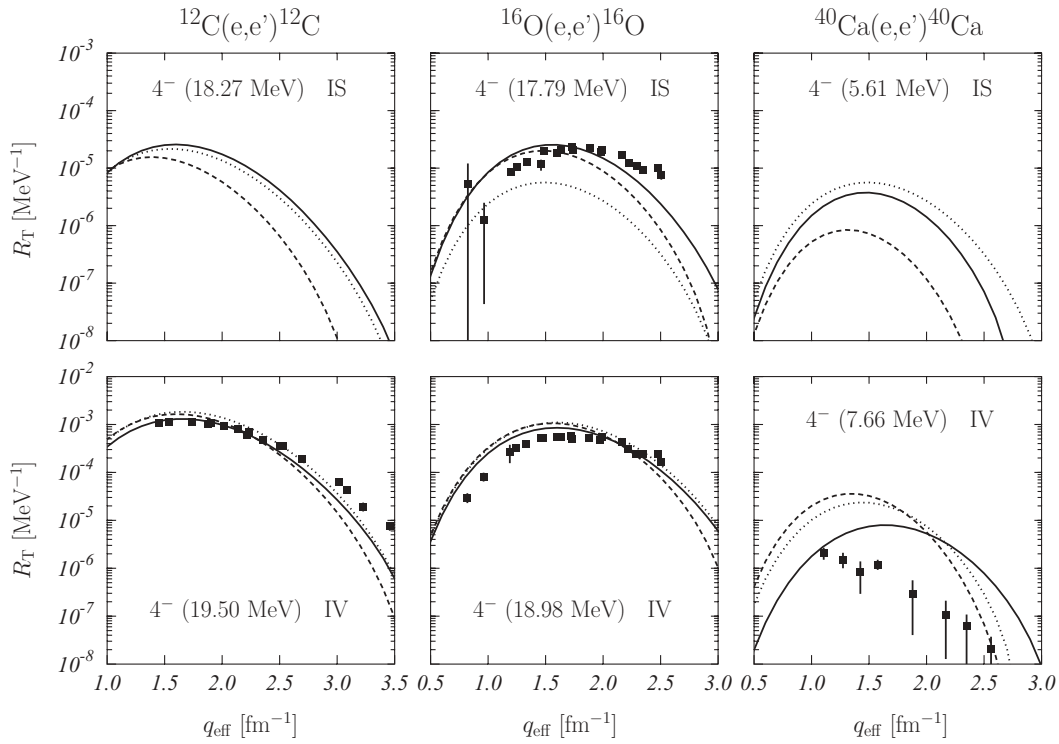

FIG. 12. Electromagnetic responses of some 4$^-$ isospin doublets. The meaning of the lines is the same as in Fig. 11. Also, the low-energy D1 responses are plotted together with the high-energy phenomenological responses, and vice versa.

We start our discussion with the 1$^+$ isospin doublet in ^{12}C, whose electromagnetic responses are shown in Fig. 11. The striking result is that when the D1 interaction is used, the position of the IS and IV states is inverted. In the self-consistent calculations with the D1 interaction, we obtain the lowest 1$^+$ state at 7.72 MeV. In Fig. 11, the response obtained with the RPA amplitudes of this state is presented in the lower panel, together with the data and with the phenomenological response for the IV state. The self-consistent response obtained with the D1 interaction at 10.66 MeV is shown in the upper panel of the figure, together with the IS phenomenological response.

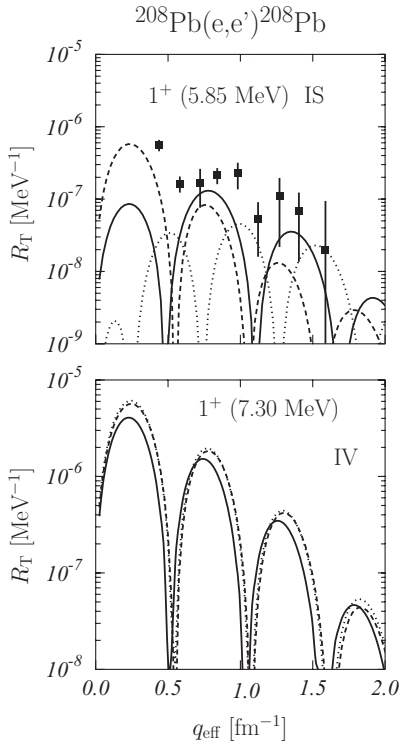

FIG. 13. Same as Fig. 11, but for the 1$^+$ isospin doublet in ^{208}Pb.

We obtain this inversion also in the calculations done with the D1 interaction and the phenomenological single-particle wave functions and energies (dotted curves). The response function of the lowest energy state, at 3.85 MeV, is shown in the lower panel together with the IV data. In the upper panel of the figure, we show the response obtained by using the RPA amplitude of the state at 8.12 MeV. It is not simple to identify the IS state among those we have obtained in this energy region. We have chosen the state showing large values of the RPA amplitude for the $[(1p_{1/2})(1p_{3/2})^{-1}]$ proton and neutron transitions. The shape of this response is very different from that of the other responses and from the data.

We found the inversion of the IS and IV partner states in all the cases we investigated. Examples are shown in Fig. 12 for a set of 4$^-$ states and in Fig. 13 for the 1$^+$ states in ^{208}Pb.

The energies, in MeV, of the self-consistent calculations of the 4$^-$ states are 1.64 and 18.64 for ^{12}C, 15.49 and 18.81 for ^{16}O, and 7.59 and 7.83 for ^{40}Ca. The comparison with the phenomenological results and with the experimental data is always done by associating the responses corresponding to the higher energy values with the IS states, and those corresponding to lower energy with the IV states. The energies of the ^{208}Pb 1$^+$ states are 6.75 MeV (IV) and 9.40 MeV (IS).

We stress that the inversion is obtained in both types of RPA calculations done with the D1 interaction, and therefore it does not depend on the single-particle basis, but it is related to the characteristics of the interaction itself. We repeated our calculations with another Gogny-like force with different values of the parameters, the D1S interaction [52], and also observed the inversion of the isospin partner states.

V. CONCLUSIONS

We have studied the magnetic excitation spectrum of doubly-closed nuclei to investigate the properties of the spin, spin-isospin, and tensor terms of the effective interaction. In a phenomenological approach, where the single-particle basis is obtained by using Woods-Saxon wells, we introduced four different interactions that reproduce the energy of specific magnetic excited states in ^{12}C, ^{16}O, ^{40}Ca, ^{48}Ca, and ^{208}Pb with the same accuracy. We first considered a zero-range interaction having only the four central channels, and we then progressively complicated the structure of the interaction by adding tensor terms and a finite range. The RPA calculations done for a large number of magnetic excitations indicate that all four interactions are able to describe with reasonable accuracy the experimental spectra and, to a lesser extent, the electromagnetic responses. We found, and pointed out, a few cases where the role of the finite range and the tensor terms is relevant, for example, the neutronic 12^- state of ^{208}Pb shown in Fig. 7.

In some cases, we found large disagreement between our calculations and the experimental data, as, for example, for the 4^- state of ^{40}Ca at 7.66 MeV, shown in Fig. 5. In these cases, however, the discrepancies between calculations and data are more related to the inadequacy of the RPA description than to a bad parametrization of the interaction.

The validity of our approach was then tested with the Gogny D1 interaction, for which we repeated the calculations of the magnetic excitation of all the states considered in the phenomenological approach. The calculations were done both using the same single-particle basis employed in the phenomenological case and in a fully self-consistent approach, where the single-particle basis was generated by a HF calculation. The striking result we obtained is that the D1 interaction inverts the energy sequence of isospin partner excitations, independent of the single-particle basis adopted and for all the nuclei studied. For a fixed multipolarity, the experimental evidence is that the IS excitation has lower energy than the IV one, while this order is inverted in the RPA calculations with the D1 interaction. Nuclear matter studies of the pairing gap done with the D1 interaction indicate anomalous behavior in the isospin $T = 0$ channel [53]. The two problems could be related. In these circumstances, the role of both the spin orbit and the residual Coulomb terms of the interaction, which are neglected in our RPA calculations, should be investigated to control the validity of the D1-like interactions for this kind of calculation.

Improvements of Gogny-like interactions have recently attracted a lot of attention [54–56], because self-consistent calculations have a wider predictive power than phenomenological approaches. The description of exotic nuclei, which will be produced and studied in future nuclear physics facilities, requires the use of well-grounded self-consistent calculations. We think that the analysis of the magnetic spectra and their electromagnetic properties is an important filter for selecting the nucleon-nucleon interactions to be used in effective nuclear theories.

ACKNOWLEDGMENTS

This work was partially supported by the Spanish Ministerio de Ciencia e Innovación under Contract FPA2008-04688 and by the Junta de Andalucía (FQM0220).

[1] J. Heisenberg and H. P. Blok, Annu. Rev. Nucl. Part. Sci. **33**, 569 (1983).
[2] T. W. Donnelly, J. D. Walecka, I. Sick, and E. B. Hughes, Phys. Rev. Lett. **21**, 1196 (1968).
[3] J. Lichtenstadt, J. Heisenberg, C. N. Papanicolas, C. P. Sargent, A. N. Courtemanche, and J. S. McCarthy, Phys. Rev. C **20**, 497 (1979).
[4] R. S. Hicks, J. B. Flanz, R. A. Lindgren, G. A. Peterson, L. W. Fagg, and D. J. Millener, Phys. Rev. C **30**, 1 (1984).
[5] S. Müller *et al.*, Phys. Rev. Lett. **54**, 293 (1985).
[6] J. E. Wise *et al.*, Phys. Rev. C **31**, 1699 (1985).
[7] T. N. Buti *et al.*, Phys. Rev. C **33**, 755 (1986).
[8] R. S. Hicks, R. L. Huffman, R. A. Lindgren, G. A. Peterson, M. A. Plum, and J. Button-Shafer, Phys. Rev. C **36**, 485 (1987).
[9] C. E. Hyde-Wright *et al.*, Phys. Rev. C **35**, 880 (1987).
[10] J. Connelly *et al.*, Phys. Rev. C **45**, 2711 (1992).
[11] G. Co' and A. M. Lallena, Nucl. Phys. **A510**, 139 (1990).
[12] A. M. Lallena, Phys. Rev. C **48**, 344 (1993).
[13] A. M. Lallena, Nucl. Phys. **A615**, 325 (1996).
[14] A. Migdal, *Theory of Finite Fermi Systems and Applications to Atomic Nuclei* (Interscience, London, 1967).
[15] J. Speth, E. Werner, and W. Wild, Phys. Rep. **33**, 127 (1977).
[16] D. Gogny, in *Nuclear Self-Consistent Fields*, edited by G. Ripka and M. Porneuf (North-Holland, Amsterdam, 1975).
[17] J. P. Blaizot and D. Gogny, Nucl. Phys. **A284**, 429 (1977).
[18] J. Dechargè and D. Gogny, Phys. Rev. C **21**, 1568 (1980).
[19] F. Arias de Saavedra, C. Bisconti, G. Co', and A. Fabrocini, Phys. Rep. **450**, 1 (2007).
[20] G. Co' and A. M. Lallena, Nuovo Cimento A **111**, 527 (1998).
[21] A. R. Bautista, G. Co', and A. M. Lallena, Nuovo Cimento A **112**, 1117 (1999).
[22] V. De Donno, Ph.D. thesis, Università del Salento, 2008.
[23] R. M. Laszewski and J. Wambach, Comments Nucl. Part. Phys. **14**, 321 (1985).
[24] R. B. Wiringa, V. G. J. Stoks, and R. Schiavilla, Phys. Rev. C **51**, 38 (1995).
[25] T. de Forest Jr. and J. Walecka, Adv. Phys. **45**, 365 (1966).
[26] S. Boffi, C. Giusti, F. Pacati, and M. Radici, *Electromagnetic Response of Atomic Nuclei* (Clarendon, Oxford, 1996).
[27] G. Co' and S. Krewald, Nucl. Phys. **A433**, 392 (1985).
[28] J. E. Amaro, G. Co', and A. M. Lallena, Ann. Phys. (NY) **221**, 306 (1993).

[29] J. S. Dehesa, S. Krewald, A. M. Lallena, and T. Donnelly, Nucl. Phys. **A436**, 573 (1985).
[30] *Table of Isotopes, 7th ed.,* edited by C. M. Lederer and V. S. Shirley (Wiley, New York, 1978).
[31] N. Y. Agafonova *et al.*, Astroparticle Physics **27**, 254 (2007).
[32] E. Kolbe, K. Langanke, and S. Krewald, Phys. Rev. C **49**, 1122 (1994).
[33] E. Kolbe, K. Langanke, F. K. Thielemann, and P. Vogel, Phys. Rev. C **52**, 3437 (1995).
[34] C. Volpe, N. Auerbach, G. Colò, T. Suzuki, and N. Van Giai, Phys. Rev. C **62**, 015501 (2000).
[35] G. Co', Acta Phys. Pol. B **37**, 2235 (2006).
[36] G. Co', V. De Donno, and C. Maieron, Nucl. Phys. B, Proc. Suppl. **188**, 136 (2009).
[37] C. Athanassopoulos *et al.*, Phys. Rev. C **58**, 2489 (1998).
[38] A. Aguilar *et al.*, Phys. Rev. D **64**, 112007 (2001).
[39] K. Eitel *et al.*, Nucl. Phys. B, Proc. Suppl. **77**, 212 (1999).
[40] F. Krmpotić, A. Samana, and A. Mariano, Phys. Rev. C **71**, 044319 (2005).
[41] A. C. Hayes, P. Navrátil, and J. P. Vary, Phys. Rev. Lett. **91**, 012502 (2003).
[42] C. F. Williamson *et al.*, unpublished.
[43] W. Steffen *et al.*, Nucl. Phys. **A404**, 413 (1983).
[44] J. E. Amaro and A. M. Lallena, Phys. Lett. **B261**, 229 (1991).
[45] J. E. Amaro and A. M. Lallena, Mod. Phys. Lett. A **7**, 3029 (1992).
[46] J. Speth, V. Klemt, J. Wambach, and G. E. Brown, Nucl. Phys. **A343**, 382 (1980).
[47] S. Krewald and J. Speth, Phys. Rev. Lett. **45**, 417 (1980).
[48] A. M. Lallena, Nucl. Phys. **A489**, 70 (1988).
[49] N. M. Hintz, A. M. Lallena, and A. Sethi, Phys. Rev. C **45**, 1098 (1992).
[50] T. Sil, S. Shlomo, B. K. Agrawal, and P. G. Reinhard, Phys. Rev. C **73**, 034316 (2006).
[51] P. Ring and P. Schuck, *The Nuclear Many-Body Problem* (Springer, Berlin, 1980).
[52] J. F. Berger, M. Girod, and D. Gogny, Comput. Phys. Commun. **63**, 365 (1991).
[53] E. Garrido, P. Sarriguren, E. Moya de Guerra, and P. Schuck, Phys. Rev. C **60**, 064312 (1999).
[54] T. Otsuka, T. Matsuo, and D. Abe, Phys. Rev. Lett. **97**, 162501 (2006).
[55] F. Chappert and M. Girod, Int. J. Mod. Phys. E **15**, 339 (2006).
[56] T. Otsuka and D. Abe, Prog. Part. Nucl. Phys. **59**, 425 (2007).